ARCHIVIO ISTITUZIONALE
DELLA RICERCA

Alma Mater Studiorum Università di Bologna
Archivio istituzionale della ricerca

Pulsed electric fields processing of apple tissue: Spatial distribution of electroporation by means of magnetic resonance imaging and computer vision system

This is the final peer-reviewed author's accepted manuscript (postprint) of the following publication:

Published Version:

Availability:
This version is available at: https://hdl.handle.net/11585/628143 since: 2021-11-03

Published:

DOI: http://doi.org/10.1016/j.ifset.2018.02.010

Terms of use:

Some rights reserved. The terms and conditions for the reuse of this version of the manuscript are specified in the publishing policy. For all terms of use and more information see the publisher's website.

This item was downloaded from IRIS Università di Bologna (https://cris.unibo.it/).
When citing, please refer to the published version.

(Article begins on next page)

20 April 2024

Accepted Manuscript

Pulsed electric fields processing of apple tissue: Spatial distribution of electroporation by means of magnetic resonance imaging and computer vision system

Nicolò Dellarosa, Luca Laghi, Luigi Ragni, Marco Dalla Rosa, Angelo Galante, Brigida Ranieri, Tiziana Marilena Florio, Marcello Alecci

PII: S1466-8564(17)30747-6
DOI: https://doi.org/10.1016/j.ifset.2018.02.010
Reference: INNFOO 1930

To appear in: *Innovative Food Science and Emerging Technologies*

Received date: 5 July 2017
Revised date: 8 February 2018
Accepted date: 11 February 2018

This is the final peer-reviewed accepted manuscript of: Nicolò Dellarosa, Luca Laghi, Luigi Ragni, Marco Dalla Rosa, Angelo Galante, Brigida Ranieri, Tiziana Marilena Florio, Marcello Alecci, Pulsed electric fields processing of apple tissue: Spatial distribution of electroporation by means of magnetic resonance imaging and computer vision system. *Innovative Food Science and Emerging Technologies, https://doi.org/10.1016/j.ifset.2018.02.010*

© 2018 Elsevier. This manuscript version is made available under the Creative Commons Attribution-NonCommercial-NoDerivs (CC BY-NC-ND) 4.0 International License (http://creativecommons.org/licenses/by-nc-nd/4.0/)

Title

Pulsed electric fields processing of apple tissue: spatial distribution of electroporation by means of magnetic resonance imaging and computer vision system

Authors and affiliations

Nicolò Dellarosa[a], Luca Laghi[a,b], Luigi Ragni[a,b], Marco Dalla Rosa[a,b], Angelo Galante[c,d,e], Brigida Ranieri[c,d], Tiziana Marilena Florio[c,d], Marcello Alecci[c,d,e]

[a] Department of Agricultural and Food Sciences, University of Bologna, Cesena, Italy

[b] Interdepartmental Centre for Agri-Food Industrial Research, University of Bologna, Cesena, Italy

[c] Department of Life, Health and Environmental Sciences, University of L'Aquila, L'Aquila, Italy

[d] National Institute for Nuclear Physics, Gran Sasso National Laboratory (INFN-LNGS), Assergi, Italy

[e] Institute SPIN-CNR, Department of Physical and Chemical Sciences, L'Aquila, Italy

Corresponding author

Luca Laghi (l.laghi@unibo.it)

Keywords

PEF; Computer vision system; Vacuum impregnation; Electroporation distribution; Magnetic resonance imaging; Relaxation times.

ABSTRACT

The optimal application of Pulsed Electric Fields (PEF) technology, used by food industry to assist mass transfer processes, depends on the effectiveness of the induced electroporation. The present work aimed at exploring the application of Magnetic Resonance Imaging (MRI) combined with Computer Vision System (CVS) analysis to assess the spatial distribution of electroporation in apple tissue. PEF-treated apple samples were compared with Dipping (Dip) and Vacuum Impregnation (VI) to gain insight into the spatial distribution of mechanisms that lead to microstructural modifications over time.

CVS showed that electroporation modified heterogeneously apple microstructure, causing enzymatic browning unevenly across the samples. MRI transverse relaxation times (T_2) maps and longitudinal relaxation times (T_1)-weighted images throughout apple tissue confirmed the inhomogeneous distribution and extent of the cell disruption, along with the release of intracellular content toward the external solution.

Industrial relevance: The novel applications of pulsed electric fields require fast and reliable methods to detect and estimate the breakage of the membranes integrity in order to boost their industrial adoption and optimization. The present study provided analytical tools able to monitor the spatial distribution of electroporation in plant tissue samples within minutes and consequently to speed up and improve the assessment of different PEF treatments.

ABBREVIATIONS

ANOVA, Analysis of variance

BW, Bandwidth

CIELab, International Commission on Illumination colour space

CVS, Computer vision system

Dip, Dipping

DSV, Diameter spherical volume

FLASH, Fast low angle shot

FOV, Field of view

GE, Gradient echo

LUT, Lookup table

MRI, Magnetic resonance imaging

MSME, Multi slice multi echo

NEX, Number of excitations

NSPEC, Single pulse sequence

PEF, Pulsed electric fields

PPO, Polyphenol oxidase

RARE, Rapid imaging with refocused echoes

RAREVTR, Rapid imaging with refocused echoes with variable repetition time

RF, Radio frequency

ROI, Region of interest

T_1, Longitudinal relaxation time

T_2, Transverse relaxation time

TACQ, Total acquisition time

TE, Echo time

tp, Pulse length

TR, Repetition time

VI, Vacuum impregnation

1. Introduction

Pulsed electric field (PEF) technology is an innovative process with a growing interest in the food sector for many potential purposes, mainly related to the microbial inactivation and the enhancement of mass transfer. The application of high electric fields induces the breakage of plasma membranes, also known as electroporation, which can be exploited to increase the efficiency of several food processes, for instance juice extraction (Praporscic, Lebovka, Vorobiev, & Mietton-Peuchot, 2007), air and osmotic dehydration (Traffano-Schiffo, Tylewicz, Castro-Giraldez, Fito, Ragni, & Dalla Rosa, 2016; Wiktor, Iwaniuk, Śledź, Nowacka, Chudoba, & Witrowa-Rajchert, 2013) or extraction of valuable compounds (Luengo, Condón-Abanto, Álvarez, & Raso, 2014; Parniakov, et al., 2015). In general, when the electric field exceeds a critical value, membranes break down and, in case the field strength is far higher than such threshold, electroporation becomes irreversible (Donsì, Ferrari, & Pataro, 2010). In fact, the extent of electroporation is strongly affected by several treatment parameters, the accurate control of which is fundamental for the correct implementation of PEF in food industry. Particularly, electric field strength, shape, duration, number and frequency of pulses have an effect on electroporation (Barba, et al., 2015).

Screening methods based on several physical approaches have been proposed to directly estimate the extent of electroporation, especially in its irreversible form, and consequently to optimize the novel industrial PEF applications. Those procedures include the evaluation of the electrical impedance (Lebovka, Bazhal, & Vorobiev, 2002), optical (Fincan & Dejmek, 2002), acoustic (Wiktor, et al., 2016) or magnetic (Dellarosa, Ragni, Laghi, Tylewicz, Rocculi, & Dalla Rosa, 2016b) properties of the plant material. Furthermore, the assessment of effects induced by electroporation, for instance changes of colour and texture (Lebovka, Praporscic, & Vorobiev, 2004), release of specific compounds (Luengo, Álvarez, & Raso, 2013) or metabolic response (Dellarosa, Tappi, Ragni, Laghi, Rocculi, & Dalla Rosa, 2016), aims at indirectly evaluating the extent of electroporation by means of appreciable variations of relevant food features.

The above-mentioned tools are able to detect quantitatively the effects of electroporation in various matrices, but, unfortunately, they are not capable to monitor its spatial distribution through the treated tissue. Indeed, the assessment of the spatial distribution of the electric field strength is fundamental to

assure the effectiveness of the process, especially when the enhancement of mass transfer is the main target of the PEF treatment. Generally, two approaches are considered, and often combined, to overcome this lack of knowledge. On one hand, the simulation of the process by means of finite element methods is particularly tailored to design the treatment chambers for liquids (Buckow, Schroeder, Berres, Baumann, & Knoerzer, 2010). On the other hand, the use of non-destructive imaging techniques, such as magnetic resonance imaging (MRI), can provide indirect information to spatially characterize the electroporation through solid plant tissues. In the latter case, a recent innovative work focusing on potato (Kranjc, Bajd, Serša, de Boevere, & Miklavčič, 2016) showed that magnetic resonance electrical impedance tomography technique can detect the electric field distribution during the application of the pulses, while quantitative information on the induced membrane breakage could be obtained by observing the modification of the transverse relaxation time (T_2).

The present work aims at exploring the spatial distribution of electroporation in apple tissue by combining computer vision system (CVS) analysis with MRI methods. PEF treatment parameters (60 pulses, 10 µs pulse width, 100 Hz, from 100 to 400 V/cm) were chosen according to earlier studies in apple (Dellarosa, Ragni, Laghi, Tylewicz, Rocculi, & Dalla Rosa, 2016a) to obtain reversible and irreversible electroporated apple samples. MRI analysis was aided with the use of a $FeCl_3$ contrast agent solution which demonstrated to passively diffuse through plasma membranes only if electroporation took place (Dellarosa, Ragni, et al., 2016b). An initial optimization step was required to establish suitable MRI sequences and parameters in order to both optimise the spatial resolution and simultaneously reduce the experimental acquisition time to few minutes. This led to observe, for the first time, kinetic alterations of apple tissue as a function of the electroporation from 15 to 60 minutes after PEF treatments. Afterward, to understand finely the effects of pulsed electric fields on mass transfer mechanisms, T_2 maps and T_1-weighted MRI images were acquired. The obtained images were finally compared to untreated dipped apple tissue and vacuum impregnated tissues, in order to clarify the tissue alterations induced by the application of PEF technologies (Donker, Van As, Snijder, & Edzes, 1997).

2. Material and methods

2.1 Raw material

Apples (*Malus domestica*, cv Cripps Pink) were acquired at a local market and stored at 2 ± 1 °C for no longer than 6 weeks until utilization. The average moisture and soluble solid contents of apples were, respectively, 85.2 ± 0.3 g and 12.6 ± 0.3 g per 100 g of fresh product (g_{fw}). Parenchyma apple tissue samples were manually cut with a sharp cork borer and a knife to obtain cylindrical samples of 14 mm diameter and 25 mm length.

2.2 Pulsed electric field (PEF) treatments and samples processing

PEF treatments were applied to the samples by means of an in-house developed pulse generator based on metal-oxide-semiconductor field-effect transistor technology. The equipment provides monopolar pulses of near-rectangular shape at adjustable voltages, pulse width, frequency and duration, thus resulting in a variable number of delivered pulses and energy input. Treatments were run at 25 °C within a chamber equipped with two stainless steel electrodes with an active contact surface of 20 × 20 mm^2 and a distance between them fixed at 30 mm. Each treatment included the placement of an apple cylinder into the chamber with the two circular bases parallel to the electrodes. The chamber was filled up with tap water, having an electrical conductivity of 314 ± 4 μS/cm at 25 °C in order to match the electrical conductivity of the apple samples. This prevented further electric field inhomogeneity (for instance insulation or interface effects) due to the different material placed between the electrodes. The process parameters and conditions were chosen according to previous experiments (Dellarosa, Ragni, et al., 2016a). Briefly, 300, 750 and 1200 V were applied to give rise to average electric field strengths between the electrodes of 100, 250 and 400 V/cm, respectively. Pulse width was fixed at 100 ± 2 μs, repetition time at 10.0 ± 0.1 ms (100 Hz) and 60 pulses were delivered in each treatment. The current and voltage values were monitored using

a digital oscilloscope (PicoScope 2204a, Pico Technology, UK) connected to the PEF generator and a personal computer.

After PEF treatments, samples were quickly removed from the treatment chamber and immersed into an isotonic sucrose solution for 60 min, during which the analysis were carried out. Those used for MRI analysis were immersed into an isotonic sucrose solution with the addition of 10 mM iron (III) chloride, as contrast agent. The total amount of iron in the apple samples was determined after 60 min from immersion using the method described by Adams (1995). Briefly, 0.1-0.5 g of freeze-dried samples obtained from the whole cylinders were dissolved in 10 mL of 2.0 M HCl. After 5 min, 1 mL of filtered (0.45 μm) supernatant was collected, mixed with 1 mL of 1.5 M KSCN and the absorbance at 480 nm measured (UV-1601, Shimadzu, Japan). A 5-points calibration curve was built using iron (III) chloride solution in water to obtain concentrations spanning from 0.1 to 1 mM, which resulted in a coefficient of determination R^2 = 0.997; the analysis was performed in triplicate.

2.3 Dipping (Dip) and vacuum impregnation (VI) treatments, as references

Dipping and vacuum impregnation treatments were used as control samples applying a similar isotonic solution up to 60 min. According to a previous vacuum impregnation protocol (Betoret, Sentandreu, Betoret, Codoñer-Franch, Valls-Bellés, & Fito, 2012), samples were immersed into the solution and the pressure was lowered in a single vacuum step to the absolute value of 60 ± 10 mbar and maintained for 10 min. Afterward, the atmospheric pressure was restored and the samples were maintained immersed for 60 min.

2.4 Computer vision system (CVS)

Apple cylinders were collected after 15, 30, 45 and 60 min from PEF treatments, split into two equal parts and images were directly acquired by the computer vision system. Digitalized images were obtained by introducing the samples inside a black box under controlled lighting condition with a digital camera D7000

(Nikon, Shinjuku, Japan) equipped with a 105-mm lens AF-S VR Micro-Nikkor (Nikon, Shinjuku, Japan). Images were acquired at 16.2 megapixels with fixed exposition time 1/8 s, F-stop f/8 and ISO 100. For each electric field strength, at least 18 apple cylinders were sampled, along with dipping as control. Digitalized images were manually pre-elaborated by using GIMP 2.8 software (GNU Image Manipulation Program, 1995-2014) to obtain a centred circular region of interest (ROI) of 500-pixels diameter. ImageJ (Schneider, Rasband, & Eliceiri, 2012) was then employed to follow the effect of electroporation on the browning kinetic by evaluating the L* (lightness), a* (red and green, for positive and negative values, respectively), and b* (yellow and blue, for positive and negative values, respectively) parameters of the CIELab colour space (CIE International Commission on Illumination, 1976). A 16 colours Lookup Table (LUT) was finally applied to each parameter of the colour space to illustrate the spatial distribution of the L*, a* and b* channels upon treatments throughout the tissue. In this respect, it is worth noticing that CIELab values calculated from the CVS may differ from those obtained by standard methods based on tristimulus colorimeters due to the different acquisition tools. Variations of the L*, a* and b* values, in the present work, should therefore be considered in a relative scale, by comparing PEF treated and untreated samples.

2.5 Magnetic resonance imaging (MRI)

Fig. 1

Apple samples that underwent MRI analysis included PEF pre-treatment at 400 V/cm along with VI and Dip samples, as references. Figure 1 displays the experimental setup used for the MRI trials and examples of acquired T_2-weighted images. Briefly, each apple cylinder was fixed in the centre of a 50 mL falcon tube that was filled up with the isotonic solution containing 10 mM of $FeCl_3$ contrast agent. A small 0.5 mL falcon tube filled up exclusively with the isotonic solution containing the same contrast agent was placed aside, as external standard, in order to make it appear in the same field of view (FOV).

MRI experiments were carried out with a 2.35 T Biospec scanner (Bruker, Germany) comprising a superconducting magnet BC24/40 with a free bore of 400 mm and static field homogeneity in a 60 mm diameter spherical volume (DSV) of 0.05 ppm (half height). A gradient system BGA26 with a free bore of 257 mm provided a maximum gradient strength of 50 mT/m and a linearity better than 3 % in a 60 mm DSV. A shim set BS40 provided up to eight spherical harmonic terms with a maximum error less than 3 %. The MRI scanner was equipped with a transmit/receive birdcage radio frequency (RF) volume coil (8 rungs, internal diameter 62 mm, external diameter 120 mm, length 111 mm, Doty Scientific Inc. USA) tuned at the proton frequency of 100.33 MHz and with impedance matching better than -15 dB. This condition was checked for each sample by means of a network analyser Agilent E5061A (Agilent, USA). The RF amplifier provided a peak power of 1 kW capable of generating the 90° and 180° RF pulses. The scanner was interfaced with an HP XW4600 workstation, running a Linux operating system (RH WS4), and comprising the Bruker Paravision 4.0 software for data acquisition and processing (Brandolini et al., 2015).

First, a single pulse sequence (NSPEC) was applied to observe the Nuclear magnetic resonance (NMR) signal from the whole apple sample and the external reference with the aim to optimize magnetic field shimming (repetition time, TR = 8000 ms; flip angle = 10°; pulse length, tp = 100 µs; bandwidth, BW = 13 kHz; 2048 points; spectral width = 30 ppm; number of excitations, NEX = 1; total acquisition time, TACQ = 8 s). After the auto-shim procedure the NMR linewidth of the whole sample was about 6 ppm. Afterward, to check the position of the samples, three perpendicular fast scout gradient echo (GE) images (fast low angle shot, FLASH) were acquired with the following parameters: TR = 35 ms; echo time (TE) = 5 ms; tp = 1 ms; BW = 5.4 kHz; flip angle = 90°; FOV = 251 mm; 256 × 256 pixels; slice thickness = 3 mm; NEX = 1; TACQ = 9 s.

Axial T_1-weigthed Rapid imaging with refocused echoes with variable repetition time (RAREVTR) images were acquired to visualise the apple sample structure and to map the longitudinal relaxation time T_1 using the following parameters: TR = [100, 280, 480, 700, 960, 1300, 1700, 2200, 3000, 4600] ms, TE = 10 ms; tp = 2.25 ms; BW = 2.5 kHz; flip angle = 90°; FOV = 628 mm; 128 × 128 pixels; spatial resolution 0.5 mm/pixel, slice thickness = 3 mm; NEX = 1; TACQ = 30 min.

An asymmetric axial T_2-weigthed Multi slice multi echo (MSME) sequence was chosen to acquire MR images using a variable TE: 2D FOV of 125.7 × 31.4 mm^2, 256 × 64 pixels, spatial resolution=0.491 mm/pixel, 3 mm slice thickness. This gave rise to a signal evolution described by Eq. 1 (Brown, Cheng, Haacke, Thompson, & Venkatesan, 2014):

$$S = \rho\left(1 - exp^{\frac{-TR}{T_1}}\right) exp^{\frac{-TE}{T_2}} \quad \text{(Eq. 1)}$$

where, ρ is the proton density, T_1 and T_2 are the longitudinal and transverse relaxation time, respectively, while TR and TE are the adjustable acquisition parameters. To obtain the T_2 mapping, each MSME sequence included 52 equally spaced echoes with TE = k × 9.23 ms (k = 1, …, 52), TR = 10 s, NEX = 1 and TACQ = 8 min. Additional fast T_1-weigthed Rapid imaging with refocused echoes (RARE) images were also acquired to better visualise the apple sample structure and to study the percolation in the surrounding solution (TR = 10 s, TE = 9.23 ms, NEX = 1, TACQ = 1 min). The optimization of the two MRI pulse sequences resulted in relatively short total acquisition time: approximately 8 min for the T_2-map analysis and 1 min for the T_1-weigthed images, allowing studying the time course after treatments. The intensity of the T_1-weigthed images was scaled, by taking the average intensity of the external standard equal to 0.5, to allow a comparison of the apple samples treated with the different technologies (Dip, VI, PEF).

The RARE images at variable TR were fitted to obtain T_1-maps by means of the Bruker Paravision 4.0 software using a 3 parameters mono-exponential fitting. Finally, raw MSME data at variable TE, which are function of the 2D spatial coordinates and time, were fitted to obtain T_2-maps by means of an in-house developed R script (R Foundation for Statistical Computing, Austria) based on the Levenberg–Marquardt nonlinear least-squares' algorithm.

2.6 Statistical analysis

Significant differences between the treatments were studied by means of analysis of variance (ANOVA), followed by Tukey's multiple comparisons, implemented in R statistical software, at the significance level of

95% ($p < 0.05$). All the experiments were repeated at least three times and results were expressed as means ± standard deviation of replications.

3. Results and discussion

3.1 Visual changes detected by CVS

Fig. 2

CVS analysis was performed on the samples treated at 100, 250 and 400 V/cm PEF electric fields (n=18) and on a control sample, obtained by dipping an apple cylinder into an isotonic solution without any pre-treatment. Fig. 2 reports the three CIELab parameters obtained by image analysis along time after treatment, together with examples of their spatial distribution throughout the entire area covered by the apple sample. Untreated apple samples (time = 0) showed CIE values equal to L* = 85.0 ± 0.2, a* = -1,9 ± 0.1 and b* = 25.8 ± 0.6. Dipping in isotonic solution did not affect those values significantly over 60 min after immersion, as well as applying a PEF pre-treatment at 100 V/cm. Previous work (Dellarosa, Ragni, et al., 2016a, 2016b) demonstrated that electroporation occurred only in its reversible form at this relatively low electric field strength. In addition, that work demonstrated that the redistribution of water within subcellular organelles enhanced mass transfer. However, the present work highlighted no change in the visual quality. This double observation suggests that PEF can be adopted to increase mass transfer in processes coupled with reduced alteration of sensorial qualities, as in the case of fresh-cut productions.

Differently from samples untreated or subjected to 100 V/cm, a marked browning of the apple tissue was observed immediately after PEF treatments at 250 and 400 V/cm. From the first sampling point, acquired 15 min after PEF treatments, significant changes in all CIELab parameters were noticed, that progressed throughout the entire observation time. The browning resulted in a lower luminosity (L* value) and in an increase of redness (a* value) and yellowness (b* value). According to Dellarosa *et al.* (Dellarosa, Ragni, et al., 2016b), PEF treatments at 250 and 400 V/cm lead to the irreversible electroporation of the membranes, with the consequent loss of compartmentalization and release of the intracellular content. This includes intracellular enzymes, i.e. polyphenol oxidase (PPO), which promote the oxidation of phenolic

molecules leading to the enzymatic browning (Rocha & Morais, 2003). By considering both L* and a* values throughout the first hour after the application of PEF, it was possible to observe that 250 and 400 V/cm had different consequences on browning kinetics, probably due to a direct relationship between impact of the enzymatic process and applied energy. This suggests that the colour changes could be employed as an index of the extent of irreversible electroporation across the samples.

It is worth highlighting that all the tested PEF treatments gave rise to inhomogeneous colour distributions throughout the apple tissue over time, especially when monitored by means of the a* and b* parameters. This source of inhomogeneity could be ascribed to the different local conductivity of the apple parenchyma, leading to a heterogeneous electric field distribution within the tissue. Two considerations reinforce this conclusion. First, in a previous study (Kranjc, et al., 2016) authors found a patchy distribution of the electric field in potato tubers as a function of the tissue features, which could not be predicted by numerical simulation. Second, to minimize the sources of irregularity due to the electrodes configuration, in the present work relatively large parallel plates were used instead of needle electrodes (Raso, et al., 2016). About the configuration of the electrodes it is also noteworthy noticing that the tissue pieces were positioned in the treatment chamber with the cylinder axis orthogonal to the two plate electrodes in order to minimize any field inhomogeneity during treatments.

A second explanation of the inhomogeneous colour distributions throughout the apple tissue over time is the heterogeneous sensitivity to the treatment of the cells through the plant tissue. The latter phenomenon was indeed recently described by Chalermchat, Malangone, & Dejmek (2010), who found an important influence of the cell size, shape and orientation within the apple parenchyma exposed to PEF treatments.

According to Lebovka, et al. (2002), plant tissue subjected to irreversible PEF treatments shows an increased conductivity due to the cell damage as a function of the redistribution of water and solutes. Such redistribution, however, was not uniform across the samples, with the highest levels of inhomogeneity caused by the highest applied electric field strength. In order to clarify spatially distributed alterations of

the tissue microstructure, in the presence of the highest energy PEF pre-treatment at 400 V/cm, the apple tissue was investigated by MRI analysis.

3.2 Distribution of electroporation explored by MRI

Fig. 3

Multiparametric MRI provides an overview of the membranes breakage, since longitudinal (T_1) and transverse (T_2) relaxation time values have been demonstrated to be directly affected by electroporation (Hjouj & Rubinsky, 2010). In the present work, a $FeCl_3$ rich contrast agent solution was used to enhance the differences of T_1 and T_2 values between apple samples and the surrounding solution. Such solution was unable to passively diffuse through the structures of the tissue, as confirmed by the spectrophotometric measurement of the Fe^{3+}concentration. Fig. 3 shows its concentration after 60 minutes from the treatments, along with a fresh apple control. The concentration of Fe^{3+} in apple samples dipped in the contrast solution, including those pre-treated by PEF at any electric field strength, spanned from 7 to 10 mg per g of sample, with no significant differences among them. Those values were far higher than the native concentration of the ion (< 1 mg per g of fresh apple) and significantly lower than apple tissue subject to VI (16.0 ± 1.2 mg per g of fresh apple). Indeed, VI is recognized as a highly effective tool to enrich porous tissues, by filling the inner air space with an external solution (Zhao & Xie, 2004). Conversely, within the observed experimental time (60 min), PEF pre-treatment and dipping showed similar results. Such results suggested that the entrance of the external solution was not eased by the application of electric fields, so that the increase of the concentration of Fe^{3+} was probably due to surface phenomena only. It is worth noting that samples treated at 100 V/cm, therefore close to the critical irreversible threshold, showed the highest standard deviation among replicates, a possible consequence of inhomogeneous cell responses throughout the material to this PEF treatment.

Fig. 4

The impact of electroporation in apple tissue was successfully detected by observing the modification of T_2 values over time after treatment. Fig. 4 illustrates the T_2-maps of three PEF-treated samples at 400 V/cm during 60 min of immersion into the contrast solution. In general, T_2 decreased immediately after PEF treatment, showing consistent values throughout the observation time. On average, apple samples simply dipped into the contrast solution showed a T_2 value equal to 125 ± 10 ms. That value dropped to 119 ± 5 ms when electroporation was applied at 400 V/cm (Table 1).

Table 1

This decrease could be ascribed to the irreversible alteration of the tonoplast and plasma membranes, noticed elsewhere on similar samples (Dellarosa, Ragni, et al., 2016b), which causes the collapse of the cell vacuole and cytoplasm. The loss of compartmentalization eases the diffusion of the intracellular water and solutes toward extracellular spaces and the external solution. That redistribution of water, together with a lower water-to-solutes ratio, results in a different interaction between water/solutes/biopolymers inside the tissue, leading to a lower T_2 (Van Duynhoven, Voda, Witek, & Van As, 2010). Indeed, this finding is in agreement with previous investigations, which showed that any food process technology affecting the inner microstructure of apple systematically lowers its T_2 (Gonzalez, Valle, Bobroff, Biasi, Mitcham, & McCarthy, 2001; Hills & Remigereau, 1997; Mauro, et al., 2016).

In the present experiment, a direct comparison between PEF and VI was also achieved, interestingly the latter technology grants the complete replacement of air with the external solution without affecting the membrane integrity (Panarese, et al., 2016). VI leads to a generalized increase of T_2 (157±12 ms) and, concurrently, of proton density (data not shown). Thus, by comparing PEF with VI samples, the application

of high voltage electric fields appears to foster no diffusion of the external solution through the tissue pores.

It is worth observing that the reduction of T_2 was clearly heterogeneously distributed through the apple cylinders, with regions where T_2 was actually not influenced by PEF application. Considering the T_2-maps reported in Fig. 4, it is important to note that the azimuthal orientation of the cylindrical apple samples within the MRI scanner was randomly aligned with that used in the PEF treatment chamber, thus apparently giving different T_2 spatial distributions among the samples. Moreover, the spatial extension of the electroporated area also showed some degree of change among replicates. This is in agreement with our CVS results and previous literature (Kranjc, et al., 2016) on other plant tissues. The T_2-maps analysis reinforces the conclusion that the heterogeneity of apple parenchyma, in terms of conductivity and sensitivity to high voltage (Chalermchat, Malangone, & Dejmek 2010), played a non-negligible role in the effectiveness of the PEF treatment.

The T_2-maps displayed in Fig. 4 also directly reveal the percolation commonly induced by pulsed electric fields (Lebovka, Bazhal, & Vorobiev, 2001). This phenomenon was directly visible in sample 'a' after 30, 45 and 60 min. The average T_2 of the native contrast solution was 10 ± 1 ms, whereas higher T_2 values were clearly visible in several pixels surrounding the upper part of the T_2-maps, giving rise to an eruption-like shape. The percolation process took about 45 min to reach a steady state condition, corresponding to an average T_2 value of the surrounding solution of about 16 ± 1 ms. Simultaneously, a slight steady increase of the T_2 values of about 3 % was observed within the tissue. Further evidence of water migration toward the external solution was provided by the T_1-weigthed images shown in Fig. 5. Interestingly, PEF pre-treated apple samples showed a thin surrounding ring with a T_1 value that was comprised between the apple tissue (T_1 = 2481 ± 72 ms) and the contrast solution (T_1 = 47 ± 8 ms) after 60 min. It is important once more to highlight that the phenomenon was not equally distributed around the cylinders and its extent varied among the different repetitions, confirming the inhomogeneous effects of PEF through the material.

Fig. 5

This multi-parametric MRI study enabled highlighting the consequences of electroporation, causing loss of membrane integrity and migration of the intracellular content, within few minutes from the application of PEF. This promotes the employment of MRI analysis to estimate the extent of electroporation immediately after pulsation and to predict possible macroscopic changes which may require long time to become apparent (Hjouj, et al., 2010; Kranjc, et al., 2016). As a finding of general interest, MRI technique was found able to provide an accurate snapshot of distribution of the microstructural alterations throughout the plant tissues. A tailored MRI experimental set-up can be therefore designed to selectively monitor, as in the present work, a specific source of variability among many possible alternatives.

4. Conclusions

In this work the spatial distribution of electroporation in apple tissues induced by pulsed electric fields technology was accurately assessed by combining computer vision system and magnetic resonance imaging techniques. The loss of compartmentalization, as a consequence of the membranes breakage, resulted in a reduction of the transverse relaxation time, measured by MRI methods, and in the simultaneous trigger of the enzymatic browning, kinetically evaluated by CVS analysis. Interestingly, both tools described an inhomogeneous distribution of electroporation through the tissues, as a consequence of probable different local conductivity and sensitivity of the apple parenchyma cells to the pulsed electric fields. Moreover, kinetic MRI analysis highlighted the release of the intracellular content toward the external solution within about 45 min from treatment. The present work provided useful imaging methods able to monitor within minutes, and backwardly optimize, novel mass transfer processes assisted by pulsed electric fields.

Acknowledgments

This work was supported by the INNOFRUVE project, co-funded by the Emilia-Romagna Region through the POR FESR 2014-2020 funds (European Regional Development Fund).

FIGURE CAPTIONS

Fig. 1. Experimental setup for the MRI measurements: (A) schematic layout and (B) example of T_2-weighted MR images obtained at two TE values for the dipping (Dip), vacuum impregnation (VI) and pulsed electric field (PEF) treated (400 V/cm) apple samples.

Fig. 2. Computer vision system analysis of the Dip, as a control, and the PEF-treated (100, 150 and 400 V/cm) samples after 15, 30, 45, 60 min from treatments. (A) Examples of digitalized transverse images and the corresponding L* (lightness), a* (redness for positive values), b* (yellowness for positive values) channel signal levels through the apple tissue. (B) The mean values ± standard deviation (n=18) of the L*, a*, b* signal levels versus time.

Fig. 3. Concentration of Fe^{3+} in the whole apple samples, which underwent different treatments, after 60 minutes of immersion into the contrast solution: fresh apple (Fresh), vacuum impregnation (VI), dipping (Dip), pulsed electric fields (PEF) at various electric field strength. Results, expressed in mg per g of fresh product (g_{fw}), represent mean values ± standard deviation (n=3).

Fig. 4. T_2-maps in the transverse plane of three apple samples treated with pulsed electric fields (PEF) at 400 V/cm (60 pulses, 10 µs pulse width, 100 Hz) and sampled at 15, 30, 45 and 60 min after treatments; T_2-maps in the transverse plane of dipping (Dip) and vacuum impregnation (VI) apple samples after 60 min of immersion in the contrast solution.

Fig. 5. T_1-weigthed images in the transverse plane of three apple samples treated with pulsed electric fields (PEF) at 400 V/cm (60 pulses, 10 µs pulse width, 100 Hz) and sampled at 5 and 60 min after treatments; T_1-weigthed images of dipping (Dip) and vacuum impregnation (VI) apple samples after 60 min from the

treatments; intensities were scaled by fixing the external standard intensity (not shown) at 0.5 (a.u.); dashed lines show the diameter of samples before treatments.

REFERENCES

Adams, P. E. (1995). Determining iron content in foods by spectrophotometry. *J. Chem. Educ, 72*(7), 649.

Barba, F. J., Parniakov, O., Pereira, S. A., Wiktor, A., Grimi, N., Boussetta, N., Saraiva, J. A., Raso, J., Martin-Belloso, O., & Witrowa-Rajchert, D. (2015). Current applications and new opportunities for the use of pulsed electric fields in food science and industry. *Food Research International, 77*, 773-798.

Betoret, E., Sentandreu, E., Betoret, N., Codoñer-Franch, P., Valls-Bellés, V., & Fito, P. (2012). Technological development and functional properties of an apple snack rich in flavonoid from mandarin juice. *Innovative Food Science & Emerging Technologies, 16*, 298-304.

Brandolini, L., Cristiano, L., Fidoamore, A., De Pizzol, M., Di Giacomo, E., Florio, T. M., Confalone, G., Galante, A., Cinque, B., & Benedetti, E. (2015). Targeting CXCR1 on breast cancer stem cells: signaling pathways and clinical application modelling. *Oncotarget, 6*(41), 43375.

Brown, R. W., Cheng, Y.-C. N., Haacke, E. M., Thompson, M. R., & Venkatesan, R. (2014). *Magnetic resonance imaging: physical principles and sequence design*: John Wiley & Sons.

Buckow, R., Schroeder, S., Berres, P., Baumann, P., & Knoerzer, K. (2010). Simulation and evaluation of pilot-scale pulsed electric field (PEF) processing. *Journal of Food Engineering, 101*(1), 67-77.

Chalermchat, Y., Malangone, L., & Dejmek, P. (2010). Electropermeabilization of apple tissue: Effect of cell size, cell size distribution and cell orientation. *Biosystems engineering, 105*(3), 357-366.

CIE International Commission on Illumination (1976). Official recommendations of the International Commission on Illumination. *Paris: Commission Internationale de l'Èclairage.*

Dellarosa, N., Ragni, L., Laghi, L., Tylewicz, U., Rocculi, P., & Dalla Rosa, M. (2016a). Effect of pulsed electric fields on water distribution in apple tissue as monitored by NMR relaxometry. In *IFMBE Proceedings* (Vol. 53, pp. 355-358).

Dellarosa, N., Ragni, L., Laghi, L., Tylewicz, U., Rocculi, P., & Dalla Rosa, M. (2016b). Time domain nuclear magnetic resonance to monitor mass transfer mechanisms in apple tissue promoted by osmotic dehydration combined with pulsed electric fields. *Innovative Food Science and Emerging Technologies, 37*, 345-351.

Dellarosa, N., Tappi, S., Ragni, L., Laghi, L., Rocculi, P., & Dalla Rosa, M. (2016). Metabolic response of fresh-cut apples induced by pulsed electric fields. *Innovative Food Science and Emerging Technologies, 38*, 356-364.

Donker, H., Van As, H., Snijder, H., & Edzes, H. (1997). Quantitative 1H-NMR imaging of water in white button mushrooms (Agaricus bisporus). *Magnetic resonance imaging, 15*(1), 113-121.

Donsì, F., Ferrari, G., & Pataro, G. (2010). Applications of pulsed electric field treatments for the enhancement of mass transfer from vegetable tissue. *Food Engineering Reviews, 2*(2), 109-130.

Fincan, M., & Dejmek, P. (2002). In situ visualization of the effect of a pulsed electric field on plant tissue. *Journal of Food Engineering, 55*(3), 223-230.

Gonzalez, J. J., Valle, R. C., Bobroff, S., Biasi, W. V., Mitcham, E. J., & McCarthy, M. J. (2001). Detection and monitoring of internal browning development in 'Fuji'apples using MRI. *Postharvest biology and technology, 22*(2), 179-188.

Hills, B. P., & Remigereau, B. (1997). NMR studies of changes in subcellular water compartmentation in parenchyma apple tissue during drying and freezing. *International journal of food science & technology, 32*(1), 51-61.

Hjouj, M., & Rubinsky, B. (2010). Magnetic resonance imaging characteristics of nonthermal irreversible electroporation in vegetable tissue. *The Journal of membrane biology, 236*(1), 137-146.

Kranjc, M., Bajd, F., Serša, I., de Boevere, M., & Miklavčič, D. (2016). Electric field distribution in relation to cell membrane electroporation in potato tuber tissue studied by magnetic resonance techniques. *Innovative Food Science & Emerging Technologies, 37*, 384-390.

Lebovka, N., Bazhal, M., & Vorobiev, E. (2001). Pulsed electric field breakage of cellular tissues: visualisation of percolative properties. *Innovative Food Science & Emerging Technologies, 2*(2), 113-125.

Lebovka, N., Bazhal, M., & Vorobiev, E. (2002). Estimation of characteristic damage time of food materials in pulsed-electric fields. *Journal of Food Engineering, 54*(4), 337-346.

Lebovka, N., Praporscic, I., & Vorobiev, E. (2004). Effect of moderate thermal and pulsed electric field treatments on textural properties of carrots, potatoes and apples. *Innovative Food Science & Emerging Technologies, 5*(1), 9-16.

Luengo, E., Álvarez, I., & Raso, J. (2013). Improving the pressing extraction of polyphenols of orange peel by pulsed electric fields. *Innovative Food Science & Emerging Technologies, 17*, 79-84.

Luengo, E., Condón-Abanto, S., Álvarez, I., & Raso, J. (2014). Effect of pulsed electric field treatments on permeabilization and extraction of pigments from Chlorella vulgaris. *The Journal of membrane biology, 247*(12), 1269-1277.

Mauro, M. A., Dellarosa, N., Tylewicz, U., Tappi, S., Laghi, L., Rocculi, P., & Rosa, M. D. (2016). Calcium and ascorbic acid affect cellular structure and water mobility in apple tissue during osmotic dehydration in sucrose solutions. *Food Chemistry, 195*, 19-28.

Panarese, V., Herremans, E., Cantre, D., Demir, E., Vicente, A., Galindo, F. G., Nicolai, B., & Verboven, P. (2016). X-ray microtomography provides new insights into vacuum impregnation of spinach leaves. *Journal of Food Engineering, 188*, 50-57.

Parniakov, O., Barba, F. J., Grimi, N., Marchal, L., Jubeau, S., Lebovka, N., & Vorobiev, E. (2015). Pulsed electric field and pH assisted selective extraction of intracellular components from microalgae Nannochloropsis. *Algal Research, 8*, 128-134.

Praporscic, I., Lebovka, N., Vorobiev, E., & Mietton-Peuchot, M. (2007). Pulsed electric field enhanced expression and juice quality of white grapes. *Separation and Purification Technology, 52*(3), 520-526.

Raso, J., Frey, W., Ferrari, G., Pataro, G., Knorr, D., Teissie, J., & Miklavčič, D. (2016). Recommendations guidelines on the key information to be reported in studies of application of PEF technology in food and biotechnological processes. *Innovative Food Science & Emerging Technologies, 37*, 312-321.

Rocha, A., & Morais, A. (2003). Shelf life of minimally processed apple (cv. Jonagored) determined by colour changes. *Food Control, 14*(1), 13-20.

Schneider, C. A., Rasband, W. S., & Eliceiri, K. W. (2012). NIH Image to ImageJ: 25 years of image analysis. *Nature methods, 9*(7), 671.

Traffano-Schiffo, M., Tylewicz, U., Castro-Giraldez, M., Fito, P., Ragni, L., & Dalla Rosa, M. (2016). Effect of pulsed electric fields pre-treatment on mass transport during the osmotic dehydration of organic kiwifruit. *Innovative Food Science & Emerging Technologies, 38*, 243-251.

Van Duynhoven, J., Voda, A., Witek, M., & Van As, H. (2010). Time-domain NMR applied to food products. *Annual reports on NMR spectroscopy, 69*, 145-197.

Wiktor, A., Gondek, E., Jakubczyk, E., Nowacka, M., Dadan, M., Fijalkowska, A., & Witrowa-Rajchert, D. (2016). Acoustic emission as a tool to assess the changes induced by pulsed electric field in apple tissue. *Innovative Food Science & Emerging Technologies, 37*, 375-383.

Wiktor, A., Iwaniuk, M., Śledź, M., Nowacka, M., Chudoba, T., & Witrowa-Rajchert, D. (2013). Drying kinetics of apple tissue treated by pulsed electric field. *Drying Technology, 31*(1), 112-119.

Zhao, Y., & Xie, J. (2004). Practical applications of vacuum impregnation in fruit and vegetable processing. *Trends in Food Science & Technology, 15*(9), 434-451.

Table 1. Summary of the longitudinal (T_1) and transverse (T_2) relaxation time values for the dipping (Dip), vacuum impregnation (VI) and pulsed electric fields (PEF) at 400 V/cm measured in the surrounding liquid and the apple samples.

	Liquid		Apple	
	T_1 (ms)	T_2 (ms)	T_1 (ms)	T_2 (ms)
Dip	23 ± 5	11 ± 1	2236 ± 83	125 ± 10
VI	29 ± 7	10 ± 1	1672 ± 106	157 ± 12
PEF 400 V/cm	47 ± 8	16 ± 1	2481 ± 72	119 ± 5

Results are means ± standard deviations (n=4)

HIGHLIGHTS

- Image analysis described the pulsed electric fields-induced enzymatic browning
- T_2-maps showed the loss of compartmentalization distributed throughout the tissue
- T_2- and T_1-weigthed images showed the percolation of the intracellular content
- Inhomogeneous spatial distribution of irreversible electroporation was noticed

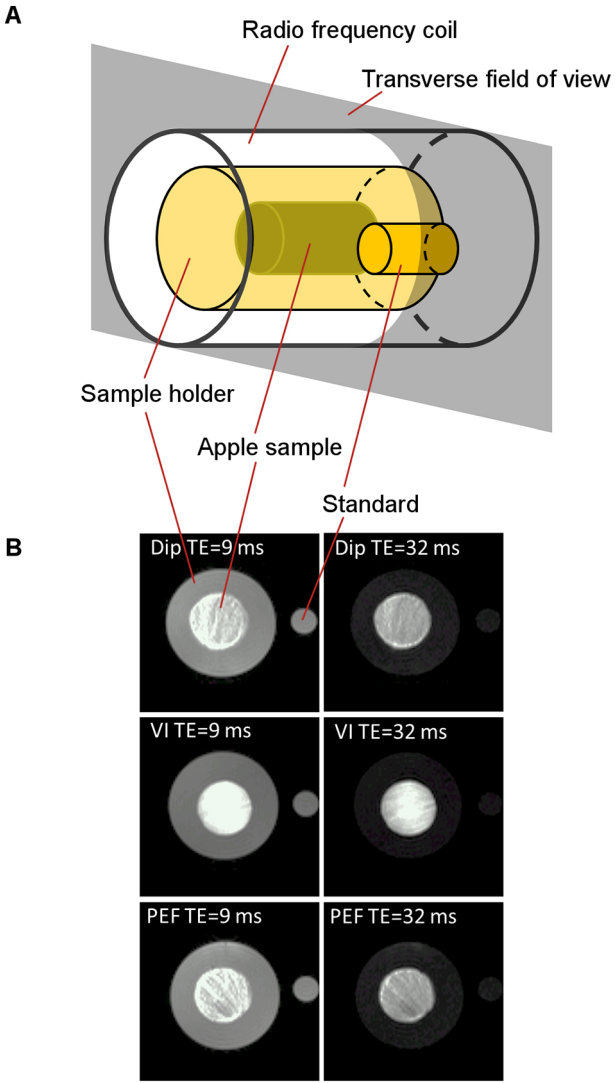
A
Radio frequency coil
Transverse field of view
Sample holder
Apple sample
Standard
B
Dip TE=9 ms
Dip TE=32 ms
VI TE=9 ms
VI TE=32 ms
PEF TE=9 ms
PEF TE=32 ms

Figure 1

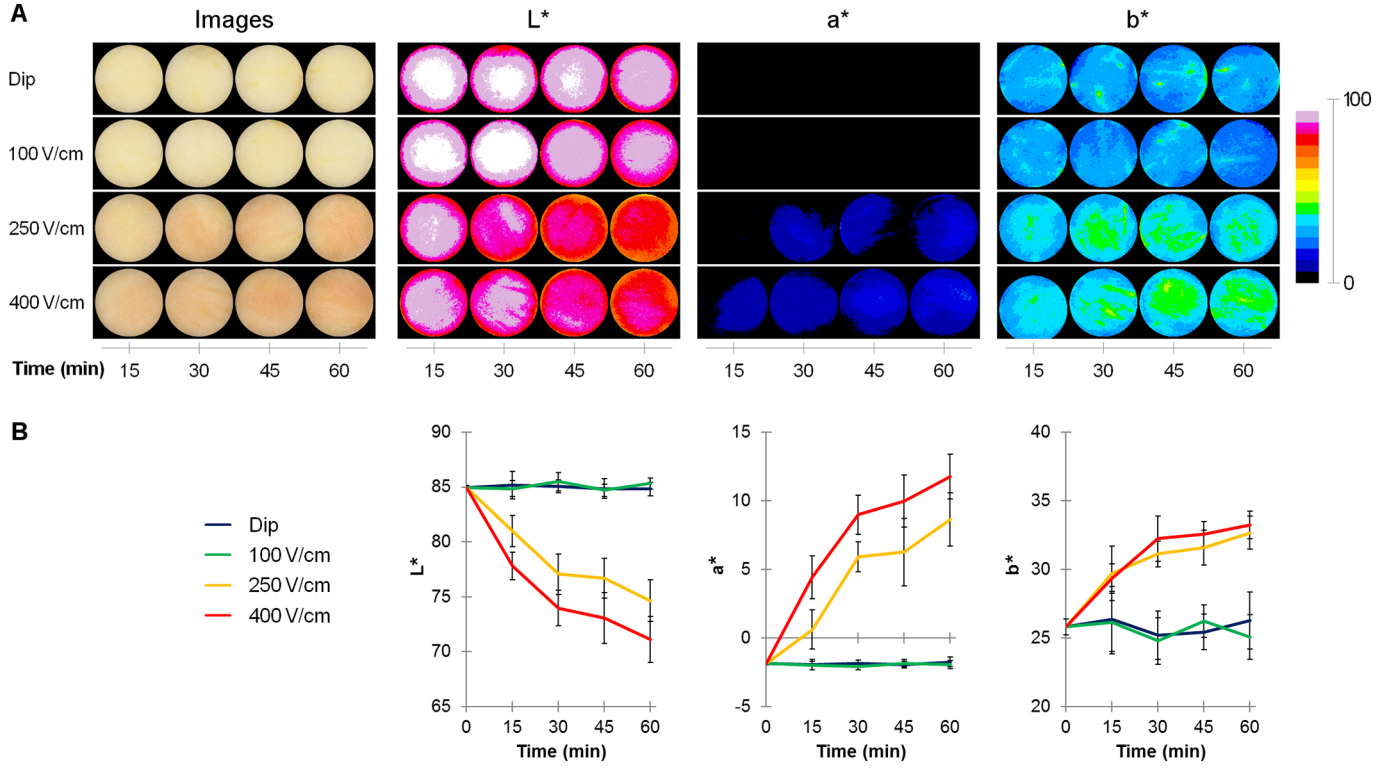
A
Images
L*
a*
b*
Dip
100 V/cm
250 V/cm
400 V/cm
Time (min) 15 30 45 60
100
0
B
Dip
100 V/cm
250 V/cm
400 V/cm
L*
a*
b*
Time (min)

Figure 2

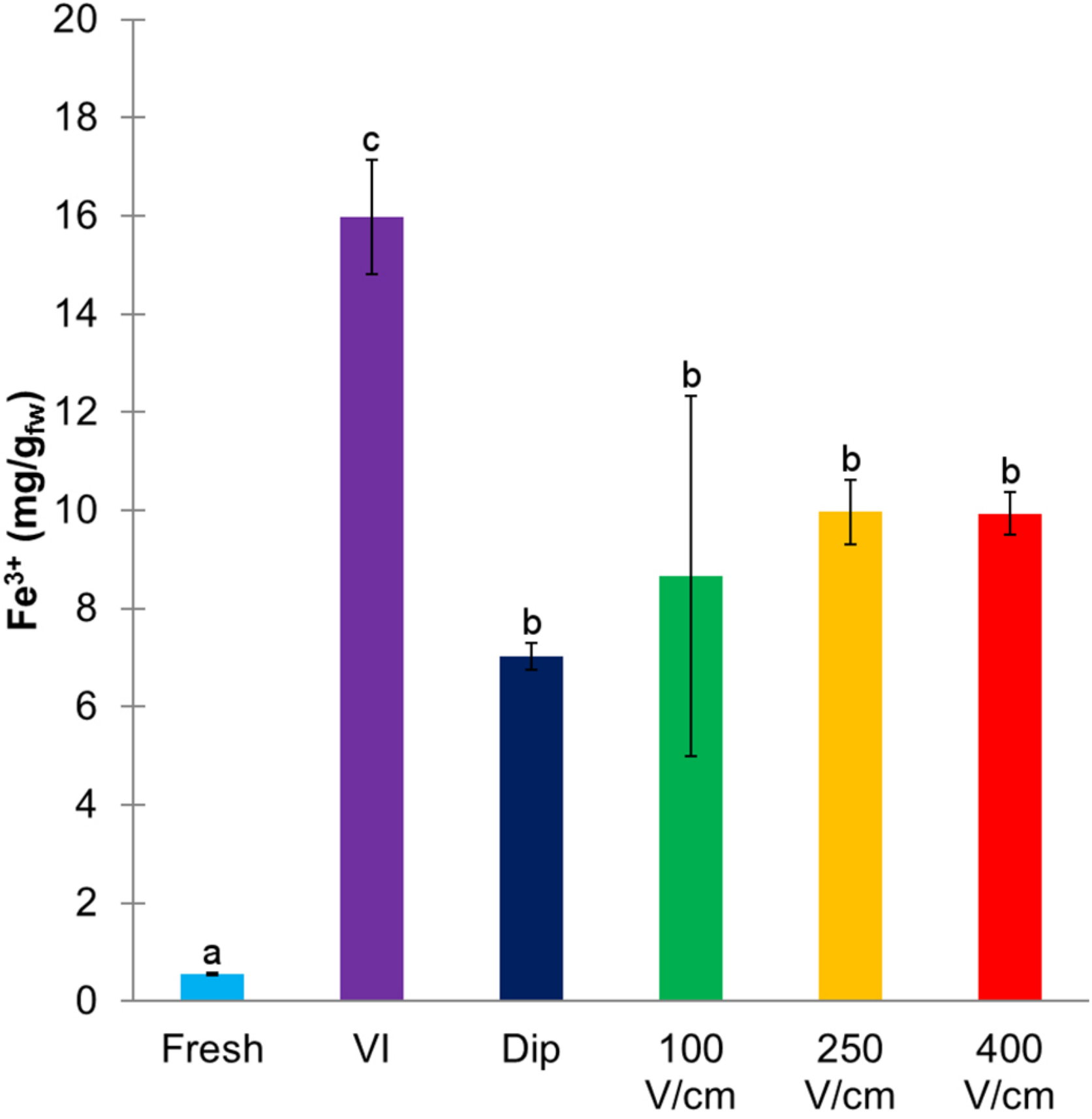
20
18
16
14
12
10
8
6
4
2
0
Fe3+ (mg/gfw)
a
c
b
b
b
b
Fresh
VI
Dip
100 V/cm
250 V/cm
400 V/cm

Figure 3

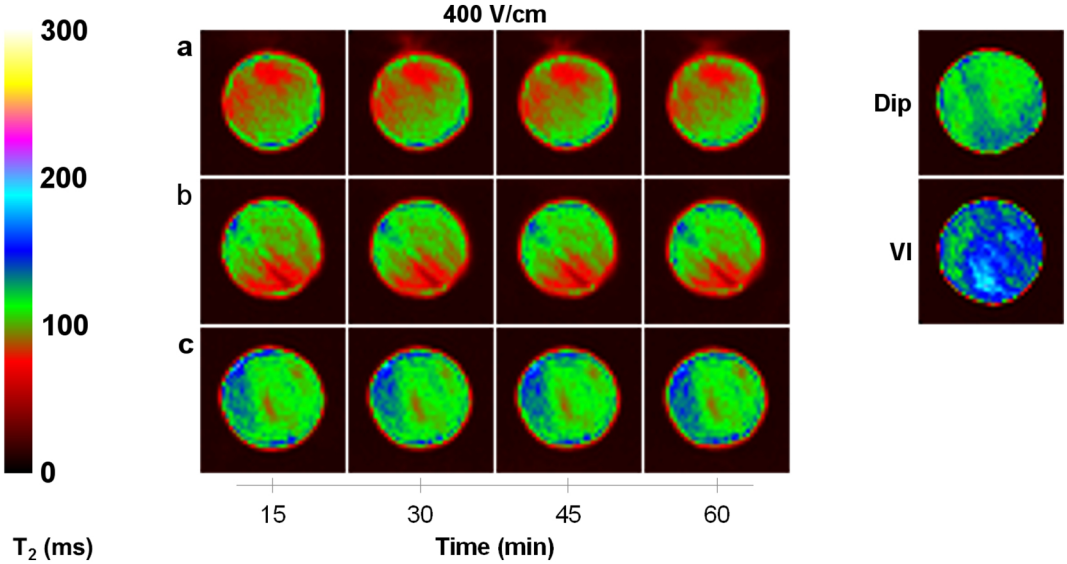

Figure 4

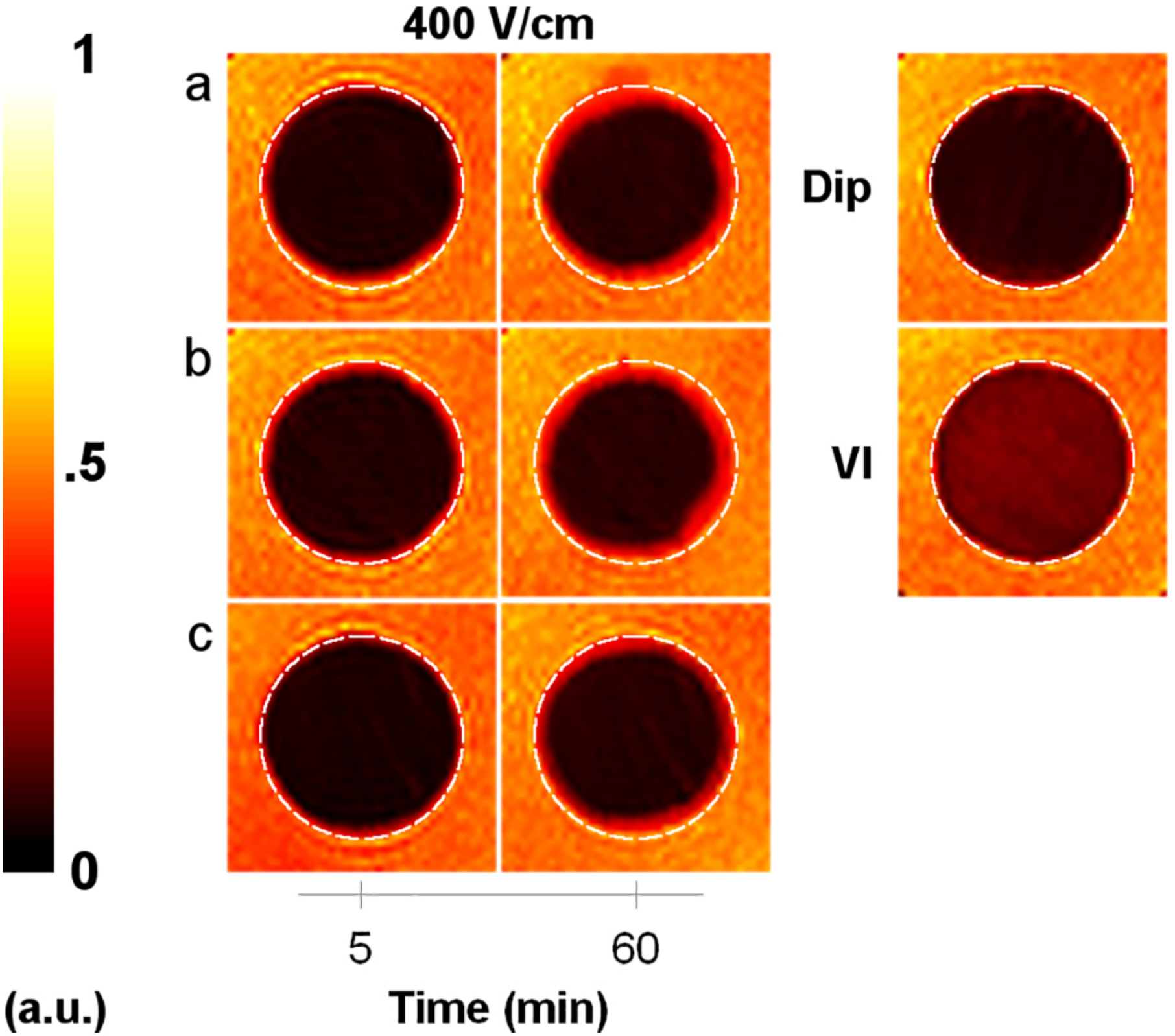

Figure 5